Impact of AS6802 synchronization protocol on time-triggered and rate-constrained traffic

Finzi, Anaïs; Zhao, Luxi

Published in:
Proceedings of 32nd Euromicro Conference on Real-Time Systems

Link to article, DOI:
10.4230/LIPIcs.ECRTS.2020.17

Publication date:
2020

Document Version
Publisher's PDF, also known as Version of record

Impact of AS6802 Synchronization Protocol on Time-Triggered and Rate-Constrained Traffic

Anaïs Finzi
TTTech Computertechnik AG, Wien, Austria
anais.finzi@tttech.com

Luxi Zhao
Technical University of Denmark, Lyngby, Denmark
luxzha@dtu.dk

Abstract

TTEthernet is an Ethernet-based synchronized network technology compliant with the AFDX standard. It supports safety-critical applications by defining different traffic classes: Time-Triggered (TT), Rate-Constrained (RC), and Best-Effort traffic. The synchronization is managed through the AS6802 protocol, which defines so-called Protocol Control Frames (PCFs) to synchronize the local clock of each device. In this paper, we analyze the synchronization protocol to assess the impact of the PCFs on TT and RC traffic. We propose a method to decrease the impact of PCFs on TT and a new Network Calculus model to compute RC delay bounds with the influence of both PCF and TT traffic. We finish with a performance evaluation to i) assess the impact of PCFs, ii) show the benefits of our method in terms of reducing the impact of PCFs on TT traffic and iii) prove the necessity of taking the PCF traffic into account to compute correct RC worst-case delays and provide a safe system.

2012 ACM Subject Classification Networks → Network performance analysis

Keywords and phrases AS6802, TTE, Modeling, Performance analysis

Digital Object Identifier 10.4230/LIPIcs.ECRTS.2020.17

1 Introduction

For safety-critical application domains, proof of the correct temporal behaviour of critical communication flows is required. For example, in the aerospace domain, but also in emerging industrial automation systems, authorities require the proof of correctness as part of the certification process with respect to critical traffic fulfilling end-to-end delay requirements. These requirements have been guaranteed through analysis methods like Network Calculus [8, 7, 6] or the more recent Compositional Performance Analysis [20], for technologies like Avionics Full DupleX (AFDX) [1]. Network Calculus [8] is a well-known mathematical framework based on min-plus algebra that is widely used in the certification process to derive worst-case end-to-end delays for individual asynchronous communication flows.

TTEthernet (SAE AS6802 [11, 16]) is a standard designed to offer strict deterministic guarantees to real-time traffic through the synchronous Time-Triggered (TT) traffic and two traffic classes of asynchronous Rate-Constrained (RC) traffic inherited from the AFDX standard. TTEthernet also considers non-time-sensitive Best-Effort (BE) traffic, and the Protocol Control Frame (PCF) traffic, which is used to keep the local clocks synchronized.

For the TT traffic class, determinism is ensured via an offline communication schedule that enforces a contention-free and precise delivery of critical frames across a switched multi-hop network within defined delay and jitter bounds. For RC traffic, determinism is ensured via a strict shaping and policing of the traffic in the devices of the network.

There are several works proposing methods to compute the RC real-time guarantees within a TTEthernet network, e.g. [15] [19] [22]. However, none consider PCF traffic, which

has the highest priority and can impact the RC delays. Consequently, the interference of PCFs on RC could impact the safety of the systems validated with the existing methods.

The synchronization is a core feature of TTEthernet. While several works have studied the synchronization protocol of TTEthernet to prove its validity [12, 18, 17], to the best of our knowledge, there has not been a study showing the impact of the synchronization protocol on TT and RC traffic.

Hence, the main contributions are threefold, we propose: i) the first formal model of the PCF traffic in Section 6; ii) the study of the PCF impact on TT and a method to mitigate such impact, i.e. *improved TT Sending Windows* in Section 7; iii) the first model to consider the impact of PCF traffic, as well as the impacts of TT and BE traffic, to compute worst-case RC delays in a formal timing analysis in Section 8.

We present the background in Section 2 and related work in Section 3. Then, the problem and our analysis strategy are formulated in Section 4. The first steps of the strategy is presenting our system model and timing analysis in Section 5. Next, we define the PCF model in Section 6. It is followed by analyses of the PCF impact on TT in Section 7 and on RC in Section 8. Finally, a performance evaluation and a conclusion are detailed respectively in Sections 9 and 10.

2 Background

2.1 Network Calculus

The timing analyses detailed in this paper are based on the Network Calculus [10]. This framework is well recognized and has been successfully used for the certification of AFDX networks [8] on the A380 and A350. It is used to compute upper bounds of delay and backlog. These bounds depend on i) the traffic arrival described by the so-called *arrival curve* $\alpha(t)$, i.e. the maximum amount of data that can arrive in any time interval, and on ii) the availability of the crossed node described by the so-called minimum *service curve* $\beta(t)$, i.e. the minimum amount of data that can be sent in any time interval.

▶ **Definition 1** (Arrival curve [10]). *$\alpha(t)$ is an arrival curve for a flow with an input cumulative function $A(t)$, i.e., the number of bits received until time t, iff: $\forall t \geqslant 0, A(t) \leqslant A(t) \otimes \alpha(t)$, with $\forall$ f, g: $f(t) \otimes g(t) = \inf_{0 \leqslant s \leqslant t}\{f(t-s) + g(s)\}$.*

▶ **Definition 2** (Minimum service curve [10]). *The function $\beta(t)$ is the minimum service curve for a data flow with an input cumulative function $A(t)$ and an output cumulative function $A^*(t)$, iff : $\forall t \geqslant 0$, $A^*(t) \geqslant A(t) \otimes \beta(t)$.*

With the definitions of the arrival and service curves, Th. 1 and Th. 2 are given to compute the main performance metrics.

▶ **Theorem 1** (Performance bounds [10]). *Consider a flow f constrained by an arrival curve α crossing a system $\mathcal{S}$ that offers a minimum service curve β. We denote v (resp. h) the maximal vertical (resp. horizontal) distance. The performance bounds at any time t are:*
Backlog: $\forall\ t:\ q(t) \leqslant v(\alpha, \beta)$; Delay: $\forall\ t:\ d(t) \leqslant h(\alpha, \beta)$
Output arrival curve: $\alpha^*(t) = (\alpha \oslash \beta)(t)$, with $\forall$ f, g: $(f \oslash g)(t) = \sup_{s \geqslant 0}\{f(t+s) - g(s)\}$

▶ **Theorem 2** (Left-over service curve - Non-Preemptive Static Priority (NP-SP) multiplexing [2]). *Consider a system with the output capacity C_{out} and m flows crossing it, f_1,f_2,..,f_m. The maximum packet length of f_i is $l_{i,max}$ and f_i is α_i-constrained. The flows are scheduled by the NP-SP policy, where priority of f_i > priority of $f_j \Leftrightarrow i > j$. For each $i \in \{1, .., m\}$, the service curve of f_i is given by: $\beta_i(t) = (C_{out} \cdot t - \sum_{j>i} \alpha_j - \max_{k<i} l_{k,max})_{\uparrow}$, with $\forall$ g: $g_{\uparrow}(t) = \left(\sup_{0 \leqslant s \leqslant t} g(s)\right)^+$, and $\forall$ x: $(x)^+ = \max(0, x)$.*

2.2 TTEthernet

The TTEthernet [9] standard is based on the use of global time synchronization to send TT frames within precise, predefined windows to ensure the lowest contention and delays. A TT flow i is defined by a maximum frame size MFS_i, period P_i and Sending Window (window during which the transmission must start and end), which starts at the offset o_i^p (the earliest time the transmission can start), in each output port p.

TTEthernet inherits the virtual link (VL) concept from the AFDX standard [1]. This concept provides a way to reserve a guaranteed bandwidth for each traffic flow. A VL represents a multicast communication from one sender to one or more receivers. Each VL is characterized by: i) a Bandwidth Allocation Gap (BAG), ranging in powers of 2 from 1 to 128 milliseconds, which represents the minimal inter-arrival time between two consecutive frames in a sender; ii) a Maximal Frame Size (MFS), ranging from 64 to 1518 bytes, which represents the size of the largest frame sent during each BAG iii) the maximum initial jitter J in the sender.

The synchronization uses the PCFs within specific VLs to keep the local clocks of all participants synchronized. These PCF flows have the highest priority in TTEthernet networks, the next priority is used by the TT flows. The next two priorities are used by the RC traffic and are denoted RC_{high} and RC_{low} respectively. The RC classes are compatible with the AFDX standard [1] and use the AFDX concept of VL. The remaining 4 lowest priorities are reserved for BE traffic.

In the next sections we present two parts of TTEthernet: the AS6802 Synchronization Protocol [11] and the TT scheduling characteristics.

2.2.1 AS6802 Synchronization Protocol

The AS6802 protocol defines three types of synchronization roles: synchronization clients (SC), synchronization masters (SM) and compression masters (CM).

The goal of AS6802 is to compensate the clock drifts and keep the difference between two clocks smaller than the synchronization *precision* of the network ϵ [17]. It is important to note that when the network is out of synchronization, no TT frame is sent. Hence, in this paper we will focus on a synchronized network, since we analyse the impact of PCFs on TT and RC.

When the network is synchronized, each SM synchronously sends PCFs to the CMs. Each CM collects the PCFs within an *acceptance window* (2 x ϵ for a fault-tolerance level 0 or 1). After the acceptance window, each CM then triggers the *compression function* computing an average between the estimated local clock drifts. Based on this average, each CM generates a frame to all SM and SC nodes at a fix offset. All SM and SC nodes will receive this PCF and correct their local clocks based on the difference between the time they expected the frame and the actual reception time. This process continues cyclically at a predefined interval called *Integration Cycle* (IC). The length of IC as well as the topology has a direct effect on the achievable synchronization precision.

2.2.2 TT scheduling

The inputs to the schedule generator are the PCF flows, TT flows, the TT flow constraints, the network constraints (see [14]). The outputs of the schedule generator are the offsets of the TT frames in each output port and the selected integration policy for each TT frame in each output port.

The goal of the TT schedule is to maximize the maximum utilization rate of the TT traffic by preventing contention between TT frames and thus minimizing the TT delays. This is achieved by computing TT Sending Windows such as they cannot overlap, and having the devices enforce the constraint that the transmission of a frame must start and end within its Sending Window. However, while this prevents contention due to other TT frames, this cannot prevent the delays due to other priority traffic:

i) higher priority shuffling delays: if frames of higher priority (i.e. PCFs) are queued in the port, the TT frame must wait until they are sent;

ii) lower priority shuffling delays: if a frame of lower priority (i.e. RC or BE) has started its transmission, a TT frame must either wait for its preemption or the end of its transmission. To manage the impact of lower priority traffic, three integration policies have been implemented: shuffling, preemption and guard band [22].

Hence, in addition to the frame transmission duration, the TT Sending Window duration may need to consider higher and lower priority shuffling. Thus, the number of PCFs impacting TT frames can have a large impact on the schedule generation.

3 Related Work

The AS6802 protocol has been studied in several works [12, 18, 17], but they have been focused on the validation of the protocol and the network precision. To the best of our knowledge, this is the first work studying the AS6802 protocol to evaluate the impact of PCF traffic on TT and RC traffic.

Concerning the evaluation of the RC delays, the earliest analysis of RC traffic [15] in TTEthernet assumes pessimistically that all RC frames in an output port of a switch will delay the current RC frame under analysis, and considers that the TT schedule contains periodically alternating phases for TT traffic and for RC traffic. However, realistic schedules do not necessarily contain such periodic phases.

Later, a Network Calculus-based analysis was proposed in [21] to compute the worst-case delays of RC frames by considering a variable size of TT frames and focusing on the shuffling integration policy. However, the protocol uses fixed-sized frames. Additionally, the preemption and guard band integration policies had not been considered in [21].

A recent analysis of RC flows in TTEthernet has been proposed in [19]. The authors use a response-time analysis based on the concept of "busy period" (time interval starting when the frame arrives at the incoming network node, and ending when the frame was transmitted on the dataflow link to the next network node). Their analysis shows that they are able to significantly reduce the pessimism compared to previous approaches. However, their analysis computes the delays for each time instant of the TT schedule, which is time-consuming. As shown in [22], their method does not scale for large problem sizes.

The most recent analysis [22] is based on Network Calculus and the analysis is done for all three integration policies. It shows good performances even compared to [19]. This work [22] considers that all frames are subject to the same integration policy. However, it is not always the case, especially when considering the shuffling and guard band policies. For instance, an implementation of the approach based on Satisfiability Modulo Theories (SMT) proposed in [14, 5] can determine if the guard band is needed and activate it for specific TT flows in specific ports.

More importantly, a common point of all these works [15, 19, 22, 21] is that none of them takes into account the impact of the PCF traffic, which may lead to optimistic RC bounds. The first work to consider PCF traffic is [3]. It focuses on the impact of the interactions

between TT and RC by changing the type of a flow between TT and RC and studying the effects of this change. Additionally, their TT Sending Windows always consider one PCF, which may not always be true, as a port can contain several PCF flows.

On the contrary, this paper considers realistic PCF traffic and studies the impact of the synchronization protocol on TT and RC traffic, while keeping fix flow types for each flow.

4 Preliminary Analysis

The main notations used in this paper are presented in Table 1. Since we are studying data transported in the network links, from now on, MFS will include the preamble, start of frame delimiter and interframe gap.

Table 1 Main notations.

PCF, TT, BE	Protocol Control Frame, Time-Triggered traffic, Best-Effort traffic
RC	Rate-Constrained traffic, composed of two priority classes: RC_{high} and RC_{low}
PTT	Policed Time-Triggered traffic (see Definition 4)
$\alpha_i^p(t)$, $\alpha_i^{*,p}(t)$	Input and output arrival curves of flow i in port p [in bits per second]
$\alpha_I^p(t)$	Input arrival curve of aggregate flow I in port p [in bits per second]
$\beta_I^p(t)$	Minimum service curve of aggregate flow of class I in port p [in bits per second]
C_{out}^p, C_{in}^p	Output and input capacities of port p [in bits per second]
MFS_i	Maximum Frame Size of frame, flow or classes i [in bits]
MFS_I^p	Maximum Frame Size of flows of classes I in port p [in bits]
BAG_i, J_i	Bandwidth Allocation Gap and initial Jitter of flow i [in seconds]
CM, SM, SC	Compression Master, Synchronization Master and Synchronization Client
ϵ	Max. synchronization error (i.e. precision) between two local clocks [in seconds]
IC, IW, SW	Integration Cycle, PCF Integration Window, TT Sending Window [in seconds]
EA, LA	Earliest and latest arrival times [in seconds]
EF, LF	Earliest and latest finish transmission times [in seconds]
o_i^p, P_i	Offset in output port p and period of flow i [in seconds]
Δ_i^p, δ_i^p	Worst-case and best-case delay of flow i in output port p [in seconds]
$\Delta_i^{[src,n]}$, $\delta_i^{[src,n]}$	Worst-case and best-case delay of flow i from source to node n [in seconds]
N_{PCF}^p	Number of PCF flows in port p
$N_{PCF,i\in TT}^p$	Number of PCF impacting TT flow i
τ^p	Hyperperiod of TT∪PCF flows in port p [in seconds] (see Eq. (5))
$N^{p,\tau}$	Total number of frames of classes PCF and TT within a hyperperiod τ^p
$f_g^{p,\tau}$, $f_{bm\oplus g}^{p,\tau}$	g-th frame within a hyperperiod τ^p, and g-th frame after frame $f_{bm}^{p,\tau}$

Our goal is to assess the impact of PCFs on TT and RC traffic and propose a method to reduce this impact.

4.1 Initial Analysis

TT traffic: PCF traffic impacts TT through the higher priority shuffling, which is part of the TT Sending Windows. Hence, by reducing the higher priority shuffling, we should be able to limit the impact of PCFs on TT.

RC traffic: PCF has a higher priority than RC and as such must be taken into account in the RC service curves (see Th. 2), which impact the RC worst-case end-to-end delays.

PCF traffic: PCFs are treated by switches as event-based (RC-like) traffic. However, similarly to TT traffic, when the network is synchronized they are generated at specific points

in time, e.g. PCFs are generated by the SCs at the beginning of each IC. Thus, knowing the best-case and worst-case delays within the network, it is possible to compute the so-called PCF Integration Window (IW), during which a PCF can be present in an output port (in the time reference of the local clock). This means the PCF traffic can only impact TT and RC inside these IWs.

In this paper, we propose to use the characteristics of the PCF traffic to minimize the impact of PCFs on TT and RC.

4.2 Mitigation and analysis strategies

Impact of PCFs on TT traffic: the *current TT Sending Window* computation consider the total number of PCF flows crossing a port, as the higher priority shuffling, regardless of the worst-case sphere of influence of PCFs on TT, i.e. IWs (see Fig. 1(a)). However, as mentioned in Section 4, outside the IWs, no PCF can interfere with a TT frame. Hence, we propose *improved TT Sending Windows* to mitigate the impact of PCFs on TT traffic, by considering the maximum number of PCFs which can impact a TT frame (see Fig. 1(b)).

The improved method is detailed in Section 7.2 by defining the constraints that must be applied when computing a TT schedule (with a heuristic scheduler [13] or SMT [14, 5] for example). The impact of PCFs on TT traffic is assessed in Section 9, using three metrics described in Section 7, i) worst-case end-to-end delay, ii) maximum jitter, and iii) reserved bandwidth.

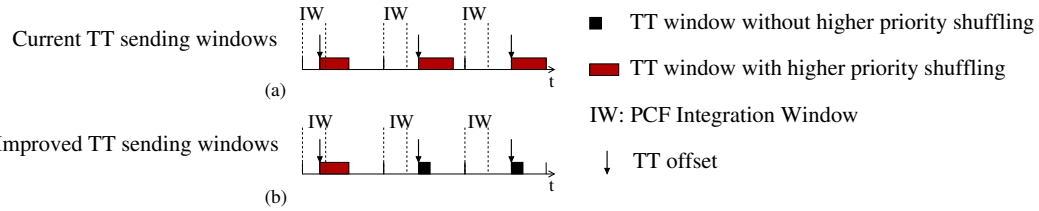

Figure 1 Strategy to mitigate the impact of PCFs on TT traffic.

Impact of PCFs on RC traffic: a direct application of Th. 2 can be done by considering PCF as an event-based (RC-like) traffic and computing the arrival curves separately from RC and TT. However, we have shown that, when the network is synchronized, the arrival times of the PCFs can be computed, similarly to TT traffic. The existing analysis in [22], of the impact on RC of TT traffic and the TT integration policies, is based on the knowledge of the TT offsets. It considers the time a TT frame arrives in an output port (i.e. is released for transmission selection by a switch) to compute a precise arrival curve. In this paper, we propose to extend the analysis to PCFs and TT traffic. Hence, the TT Sending Windows and IWs (detailed in Sections 5.4 and 6 respectively) are used together to compute the precise impact of PCF and TT on RC traffic. Thus, we compute a single arrival curve for both PTT and PCF classes, i.e. $\alpha_{PTT \cup PCF}(t)$ detailed in Section 8, in Th. 11, where PTT is a so-called Policed TT (PTT) class (detailed in Section 8, in Definition 4 and Th. 9), encompassing TT traffic and TT integration policies.

The impact of PCFs on RC traffic will be assessed in Section 9 by comparing our RC end-to-end delay results to the results of implementing the model presented in [22].

First, in the next section we present our system model and delay computation overview, which are needed to detail the computation of IW in Section 6. The IWs are in turn use in the TT mitigation method and and RC analysis in Sections 7 and 8.

5 System model and delay computation overview

5.1 Traffic model

PCF and RC traffic use VLs, so each flow i is defined by a priority, MFS_i, BAG_i and J_i. For example, the leaky bucket arrival curve for such a flow i in the source node src is:

$$\alpha^{src}_{i\in PCF\cup RC}(t) = \begin{cases} 0,\ t \leqslant 0 \\ \frac{MFS_i}{BAG_i} \cdot (t + J_i) + MFS_i,\ t > 0 \end{cases}$$

The above parameters of an RC flow are user-variables, whereas the PCF flows are described in Th. 4 in Section 6.

5.2 Device model

A device (end-system or switch) is characterized by the ports (which can be used as input and output), the forwarding process between the input port and output ports, and the priority queues. The forwarding process in a device n is characterized by known best-case and worst-case forwarding delays, denoted δ^n_{fwd} and Δ^n_{fwd}. For any switch sw, the forwarding delays are between an input port in sw (after the frame has been fully received) and the arrival in an output port in sw. For any end-system es, the forwarding delays are between i) the host in es and an output port in es (source es) or ii) an input port in es and the host in es (destination es).

5.3 Delays between a source and a device for PCF and RC

We denote $\delta_i^{[src,n]}$ (resp. $\Delta_i^{[src,n]}$) the best-case (resp. worst-case) delay of flow $i \in \{PCF, RC_{high}, RC_{low}\}$ between the source node and node n. If n is not a destination node, we consider the delay between the generation of the frame, and its arrival in the output port of n, otherwise the arrival in the destination host. For RC traffic, the source and destination nodes are end-systems. For PCF traffic, source and destination nodes can be either switches or end-systems depending on the synchronization roles.

The delay $\Delta_i^{[src,n]}$ (resp. $\delta_i^{[src,n]}$) is obtained by summing all the sources of worst-case (resp. best-case) delays along the path, which are defined as follows,

1) *delay in an input port q:* it is the reception time a frame in an input port, i.e. amount of time needed for a frame of a flow i to fully arrive in an input port q at a rate C^q_{in}: $\frac{MFS_i}{C^q_{in}}$;
2) *forwarding delays in a node n:* δ^n_{fwd} and Δ^n_{fwd} defined in Section 5.2;
3) *worst-case queuing delay Δ^p_i in an output port p:* we use Th. 1 to compute the worst-case delay bound of a flow i of class $I \in \{PCF, RC_{high}, RC_{low}\}$ in an output port p: $\Delta^p_i = h(\alpha^p_I, \beta^p_I)$, with i) the aggregate input arrival curve $\alpha^p_I(t)$ and ii) the left-over service curve $\beta^p_I(t)$, as follows:
   - **(i)** the input arrival curve $\alpha^p_i(t)$ of flow i of class I, in an output port p of device n, depends on: a) the output arrival curve exiting the preceding output port $p \ominus 1$, denoted $\alpha_i^{*,p\ominus 1}(t)$, which can be calculated using Th. 1; b) the jitter due to the forwarding delays:

$$\alpha^p_i(t) = \begin{cases} \alpha_i^{*,p\ominus 1}(t + \Delta^n_{fwd} - \delta^n_{fwd}),\ t > 0 \\ 0,\ t \leqslant 0 \end{cases} \quad (1)$$

   Then the input arrival curve of the aggregate flow of class I, $\alpha^p_I(t)$, is the sum of the input arrival curves of the flows $i \in I$ crossing p: $\alpha^p_I(t) = \sum_{i\in I, i\in p} \alpha^p_i(t)$

(ii) the service curves are computed with Th. 2. For the RC traffic, the service curves are derived when considering higher priority traffic PCF and TT together. Also, as mentioned in Section 4, the impact of the integration policies will be taken into account in the Policed TT frames (PTT), in Th. 9. Thus, in Section 8, we will consider the aggregate flow of PCF and PTT traffic, to compute the arrival curve $\alpha^p_{PTT\cup PCF}(t)$. Hence, with Th. 2, we obtain the following service curves:

$$\begin{aligned} \beta^p_{RC_{low}}(t) &= \left(C^p_{out}\cdot t - MFS^p_{BE} - \alpha^p_{RC_{high}}(t) - \alpha^p_{PTT\cup PCF}(t)\right)_{\uparrow} \\ \beta^p_{RC_{high}}(t) &= \left(C^p_{out}\cdot t - MFS^p_{BE\cup RC_{low}} - \alpha^p_{PTT\cup PCF}(t)\right)_{\uparrow} \\ \beta^p_{PCF}(t) &= \left(C^p_{out}\cdot t - MFS^p_{TT\cup RC\cup BE}\right)_{\uparrow} \end{aligned} \quad (2)$$

4) *best-case queuing delay δ^p_i in an output port p:* due to the serialization effect [7, 4], the best-case delay of flow i in a node $n \in \{es, sw\}$ is: $\delta^n_{fwd} + \frac{MFS_i}{C^p_{out}}$. When separating the node into input port, forwarding delay and queuing delay, as mentioned before, the delays for each part are considered separately. Hence, the best-case delay in output port p, i.e. with no contention and with C^q_{in} the link capacity shaping in input port q, is: $\delta^p_i = \frac{MFS_i}{C^p_{out}} - \frac{MFS_i}{C^q_{in}}$: In the source nodes, we set $C^q_{in} = +\infty$;

5) *propagation delay:* known latency on physical links.

Thus, PCF delays can now be computed, but $\alpha^p_{PTT\cup PCF}(t)$ must be defined (see Section 8) to compute RC delays.

5.4 Modeling TT Sending Windows

The size of a TT sending window is a very important parameter as it represents the impact of lower (i.e. RC and BE) and higher (i.e. PCF) priorities on TT.

▶ **Definition 3** (TT Sending Window). *A TT Sending Window $SW_{i\in TT}$ of a flow i in an output port p with an output capacity C^p_{out} is given by :*

$$SW^p_{i\in TT} = \left[EA^p_i, LF^p_i\right]$$

$EA^p_{i\in TT} = o^p_{i\in TT}$ the earliest arrival time (i.e. the offset, which is the earliest sending time);
$LF^p_{i\in TT} = EA^p_i + MFS_i/C^p_{out} + LPS^p + HPS^p_i$, i.e. the latest transmission finish time;
with LPS^p the lower priority shuffling defined in Th. 3 and HPS^p_i the higher priority shuffling defined in Th. 8.

To define the TT Sending Windows, we detail the lower priority shuffling in Th. 3 for the different integration policies. The higher priority shuffling will be defined in Th. 8 for the current computation and proposed mitigation method.

▶ **Theorem 3** (Lower priority shuffling). *The lower priority shuffling LPS^p in output port p is such as:*

$$LPS^p = \begin{cases} MFS_{RC\cup BE}/C^p_{out}, \text{ shuffling} \\ PO/C^p_{out}, \text{ preemption, with } PO \text{ the preemption overhead size} \\ 0, \text{ guard band} \end{cases}$$

Proof. With shuffling, a TT frame may be delayed until a lower priority frame finishes its transmission. Hence, a TT frame may experience the full impact of lower priority traffic.

With preemption, an interfering lower priority frame is preempted, and its transmission is restarted from the beginning after the TT frame finished transmitting. Hence, the TT frame may be delayed by the preemption time due to the preemption overhead.

With guard band, a lower priority frame is blocked (postponed) from transmission if a TT frame is scheduled to be sent before the RC frame would complete its transmission. Hence, the TT frame is not impacted by lower priority traffic. ◀

6 Modeling PCF traffic

In order to characterize the PCF traffic, we have studied AS6802 and defined Th. 4.

▶ **Theorem 4** (PCF traffic characteristics). *A PCF flow has the highest priority, and is defined by $MFS_{PCF} = 84$ bytes (incl. preamble, start of frame delimiter and interframe gap), $BAG_{PCF} = IC$, and $J_{PCF} = \epsilon$.*

Proof. The PCF traffic is assigned the highest priority [11], with MFS equals to the minimal Ethernet frame size [11]. Since one PCF is sent per flow per IC, the BAG of a PCF flow is the IC duration [11]. Concerning J_{PCF} for a PCF from either SM or CM, it is equal to ϵ:

PCF from SM to CM: the flows are generated by the SMs at the start of IC. As the maximal time drift between two clocks is lower than or equal to ϵ, the clock correction between two ICs is lower than ϵ. Hence, the initial jitter is equal to ϵ.

PCF from CM to SM and SC: for the flows sent by the CMs, a function ensures that the delays experienced by the incoming PCFs between the SMs and the CMs have no impact on the PCFs sent by the CMs. Hence, the jitter is due to the clock drift correction function. The clock drift is bounded by ϵ, thus the initial jitter is equal to ϵ. ◀

Then, to assess the presence or absence of PCFs at a time t, and the resulting impact on TT Sending Windows, we compute the IWs.

▶ **Theorem 5** (PCF Integration Window). *The PCF Integration Window of flow $i \in PCF$ in output port p of device n (i.e. when a frame of flow i can be present in p) is given by:*

$$IW^{p}_{i \in PCF} = [EA^{p}_{i}, LF^{p}_{i}] \tag{3}$$

with $EA^{p}_{i \in PCF}$ the earliest arrival time, and $LF^{p}_{i \in PCF}$ the latest finish time of transmission, of frame of flow $i \in PCF$ in output port p, such as:

$$\begin{aligned} EA^{p}_{i \in PCF} &= EA^{psrc}_{i} + \delta^{[src,n]}_{i} - \epsilon \\ LF^{p}_{i \in PCF} &= LA^{psrc}_{i} + \Delta^{[src,n]}_{i} + \Delta^{p}_{i} + \epsilon \end{aligned} \tag{4}$$

with: $\Delta^{[src,n]}_{i}$ and $\delta^{[src,n]}_{i}$, defined in Section 5.3; psrc the output port of node src in the path of flow i;

$$EA^{psrc}_{i} = \begin{cases} 0, \ PCF \ from \ SM \\ -\epsilon + MTC + \Delta CM, \ PCF \ from \ CM \end{cases}$$

$$LA^{psrc}_{i} = \begin{cases} 0, \ PCF \ from \ SM \\ +\epsilon + MTC + \Delta CM, \ PCF \ from \ CM \end{cases}$$

ΔCM, the Compression Master delay (known constant) [11]; MTC, the maximum transparent clock, a statically computed worst-case travel time of any PCF in the network.

Proof. The proof is based on i) the known sending times of the PCFs and ii) the study of the PCF delays from the source to device n. The full proof is detailed in the Appendix. ◀

7 Impacts of PCFs on TT class

In this section, we assess the impact of PCFs on TT, with and without mitigation method.

7.1 Assessing the impacts of PCFs on TT

As presented in Section 4, the PCFs impact the TT traffic through the higher priority shuffling. Hence, in Theorem 6 we present the impact of the PCFs on TT. We define the impact of PCFs on a metric as the increase of the metric due to PCFs.

▶ **Theorem 6** (PCF impacts on TT). *The PCF impact on TT is measured using three metrics i) worst-case end-to-end delay, ii) maximum jitter and iii) reserved bandwidth, as follows:*

- **i)**
  - *The maximum impact of PCF on the worst-case end-to-end delay of a flow $i \in TT$ with a path $path_i$ is: $\sum_{p \in path_i} N^p_{PCF} \cdot \frac{MFS_{PCF}}{C^p_{out}}$, where N^p_{PCF} is the number of PCF flows crossing output port p.*
  - *The minimum impact of PCF on the worst-case end-to-end delay of a flow $i \in TT$ is: $\sum_{p \in path_i} HPS^p_i$.*
- **ii)** *The impact of PCF on the maximum jitter of a flow $i \in TT$ in destination node $dest$ is: $HPS^{pdest \ominus 1}_i$, with $pdest \ominus 1$ the output port preceding node $dest$.*
- **iii)** *The impact of the PCFs on the reserved bandwidth of class TT in output port p is: $\sum_{\forall i \in TT, i \in p} \frac{HPS^p_i}{BAG_i}$.*

Proof. In each output port p of each switch n along the path $path_i$ of flow $i \in TT$, the Sending Window is scheduled after the latest arrival time of the frame in the switch (computed in Lemma 7): $o^p_i \geqslant LA^n_{i \in TT} = LF^{p \ominus 1}_i + \Delta^{p \ominus 1, n}_i + \epsilon$.

Hence, the minimum impact of PCFs on the end-to-end delay is obtained by summing the variations of $LA^n_{i \in TT}$ in each device n in the path of flow i, with PCFs versus without PCFs. Only $LF^{p \ominus 1}_i$ is impacted by the PCFs in $HPS^{p \ominus 1}_i$ (see Definition. 3). In the case of the maximum impact on the end-to-end delays, with the mitigation method, the scheduler may select offsets greater than $LA^n_{i \in TT}$ to avoid IWs. This delay is limited in each output port by the full impact of the PCFs, i.e. the transmission time of all the PCFs, which also corresponds to the impact of the PCFs for the current method.

The maximum jitter in node $dest$, $J^{dest}_{i \in TT}$, is computed using Lemma 7. As the ϵ does not impact the relative arrival times in n (since there is only one clock to consider), we obtain:
$J^{dest}_{i \in TT} = LA^{dest}_i - EA^{dest}_i - 2 \cdot \epsilon = HPS^{pdest \ominus 1}_i + LPS^{pdest \ominus 1} + \Delta^{dest}_{fwd} - \delta^{dest}_{fwd}$
with $pdest \ominus 1$ the output port preceding the destination node $dest$.

Hence, the PCFs only impact the jitter in $HPS^{dest \ominus 1}_i$.

The bandwidth reserved for each TT flow i crossing p depends on the Sending Window and is equal to $\frac{LF^p_i - EA^p_i}{BAG_i}$, which depends on the PCFs through HPS^p_i (see Definition 3). ◀

As the impact of the PCFs depends on the TT offsets constrained by the previous nodes along the path of the flow, we present next the impact of the Sending Windows in the preceding output port $p \ominus 1$, on the arrival times of flow i in a succeeding device.

It is important to note that for a TT flow, the arrival time in a device n is different from the arrival time in an output port p of n. The arrival time of a TT frame i in the device n depends on the delays after the frame was sent from the preceding output port. On the contrary, the arrival time in the output port p in device n depends on the offset of the flow i in p, i.e. when the device n releases the frame and makes it available to be selected for transmission in output port p.

▶ **Lemma 7** (Arrival time in a node). *For a flow $i \in TT$ the latest arrival time and the earliest arrival time in $n \in \{es, sw\}$ are:*

$$LA^n_{i \in TT} = LF^{p \ominus 1}_i + \Delta^{p \ominus 1, n}_i + \epsilon$$

$$EA^n_{i \in TT} = EA^{p \ominus 1}_i + \frac{MFS_i}{C^{p \ominus 1}_{out}} + \delta^{p \ominus 1, n}_i - \epsilon$$

with $LF_i^{p\ominus 1}$ *in Definition 3;* $p \ominus 1$ *the output port preceding* n*;* $EA_{i\in TT}^{p\ominus 1} = o_{i\in TT}^{p\ominus 1}$*;* $\Delta_{i\in TT}^{p\ominus 1,n} = \Delta_{prop} + \frac{MFS_{i\in TT}}{C_{out}^{p\ominus 1}} + \Delta_{fwd}^{n}$*;* $\delta_{i\in TT}^{p\ominus 1,n} = \Delta_{prop} + \frac{MFS_{i\in TT}}{C_{out}^{p\ominus 1}} + \delta_{fwd}^{n}$*;* Δ_{prop} *is the link propagation time;* δ_{fwd}^{n} *and* Δ_{fwd}^{n} *defined in Section 5.2.*

Proof. The latest (resp. earliest) arrival time is obtained by summing the delays between the latest (resp. earliest) transmission finish time in the previous node, i.e. $LF_i^{p\ominus 1}$ (resp. $EA_i^{p\ominus 1} + MFS_i/C_{out}^{p\ominus 1}$) and the arrival of the frame in n. Hence, $\Delta_{i\in TT}^{p\ominus 1,n}$ (resp. $\delta_{i\in TT}^{p\ominus 1,n}$) is the sum of the link propagation time, input port delay, forwarding delay. Due to the local clocks, ϵ is added (resp. removed) in the latest (resp. earliest) arrival time. ◀

7.2 Mitigating the impact of PCFs on TT

The method to mitigate the impact on PCFs on TT (improved TT sending windows) proposed in Section 4 is detailed as follows: the goal of this method is to limit the impact of PCFs on the TT within *HPS* (see Definition 3), by computing the number of PCFs that can impact a TT frame i, denoted $N_{PCF,i\in TT}^{p}$.

$N_{PCF,i\in TT}^{p}$ is the number of IWs opened between the earliest start of transmission, i.e. the earliest arrival time, and the latest start of transmission, due to the impact of shuffling. Hence, $N_{PCF,i\in TT}^{p}$ is the number of IWs opened within $[EA_i^p,\ EA_i^p + LPS^p + HPS_i^p]$.

Computing $N_{PCF,i\in TT}^{p}$ depends on HPS_i^p, which in turns depends on $N_{PCF,i\in TT}^{p}$. Thus, with a heuristic scheduler [13], we search for a stable value of $N_{PCF,i\in TT}^{p}$, starting at 0. With SMT [14, 5], we express the relations through first-order logic assertions.

Finally, we present the computation of the higher priority shuffling, used in Th. 6.

▶ **Theorem 8** (Higher priority shuffling). *The higher priority shuffling* HPS_i^p *of a TT flow* i *in output port* p *is such as:*

$$HPS_{i\in TT}^{p} = \begin{cases} N_{PCF}^{p} \cdot \frac{MFS_{PCF}}{C_{out}^{p}}, \text{ current TT window} \\ N_{PCF,i}^{p} \cdot \frac{MFS_{PCF}}{C_{out}^{p}}, \text{ improved TT Sending Windows} \end{cases}$$

with N_{PCF}^{p} *the number of PCF flows crossing* p*, and* $N_{PCF,i\in TT}^{p}$ *the number of IWs opened between earliest and latest start of transmission of TT flow* i*.*

Proof. Currently, the impact of higher priority shuffling on a frame $i \in TT$ in a port p always considers the total number of PCF flows crossing p. However, in Sections 4 and 7.2, we presented the improved TT Sending Windows to mitigate the impact of PCFs. Hence, HPS_i^p is equal to the transmission time of the PCFs impacting a TT frame. ◀

8 Impact of PCFs and TT on RC classes

As shown in Section 4, the impact of PCF, TT flows and TT integration policies, on RC classes is expressed in arrival curve $\alpha_{PCF\cup PTT}(t)$. We start by defining in details the PTT frames before detailing the computation of $\alpha_{PCF\cup PTT}(t)$.

8.1 Policed Time-Triggered frames

We consider the $PCF \cup TT$ flows crossing output port p. The impact of the TT integration policies is taken into account to define Policed TT frames (PTT), in Definition 4.

▶ **Definition 4** (Policed Time-Triggered Frame). *A Policed Time-Triggered (PTT) frame* $f_{g\in PTT}^{p}$ *is composed of a TT frame* $f_{g\in TT}^{p}$ *and its integration policy in output port* p*.*

To define the characteristics of PTT frames and compute the input arrival curve $\alpha_{PCF\cup PTT}(t)$ in Th. 11, we need the periodicity of the $PCF \cup TT$ flows. The behavior of the $PCF \cup TT$ flows crossing an output port p is periodic with a so-called hyperperiod τ^p such as:

$$\tau^p = LCM(P_{i\in\{PCF,TT\},i\in p}) \tag{5}$$

with LCM the least common multiple, $P_{i\in\{PCF,TT\}}$ the periods of the flows i crossing p, and $P_{i\in PCF} = BAG_{PCF}$.

For $\alpha_{PCF\cup PTT}(t)$ and the guard band policy in Th. 9, we need to characterize the earliest finish time and the arrival of the $PCF \cup TT$ flows within τ^p. We denote:

- $N^{p,\tau}$ the number of $PCF \cup TT$ frames in τ^p;
- $f_g^{p,\tau}$ the g-th frame within τ^p.

We define $f_{i(k)}^{p,\tau}$ the k-th frame of flow $i \in \{PCF, TT\}$ within τ^p with $k \in \{0, .., N_i^{p,\tau} - 1\}$, with $N_i^{p,\tau}$ the number of frames of flow $i \in \{PCF, TT\}$ in a hyperperiod τ^p. Hence, $\exists\ g \in \{0, .., N^{p,\tau} - 1\}$ such as $f_{i(k)}^{p,\tau} = f_g^{p,\tau}$. Thus, for TT and PCF, the earliest finish time, the earliest and latest arrival times of frame $f_g^{p,\tau}$ within τ^p are:

$$EA_{g\in PCF\cup TT}^{p,\tau} = EA_{i\in PCF\cup TT}^{p} + k \cdot P_i \tag{6}$$

$$LA_{g\in PCF\cup TT}^{p,\tau} = LA_{i\in PCF\cup TT}^{p} + k \cdot P_i \tag{7}$$

$$EF_{g\in PCF\cup TT}^{p,\tau} = EA_{g}^{p,\tau} + MFS_g/C_{out}^{p} \tag{8}$$

where EA_i^p and LA_i^p are the earliest and latest arrival times of flow i in an output port p.

For PCF flow i, $EA_{i\in PCF}^p$ is defined in Eq. (4), $P_{i\in PCF} = BAG_{PCF}$ and:
$LA_{i\in PCF\cup TT}^p = LF_i^p - \Delta_i^p$, with LF_i^p and Δ_i^p defined in Th. 5 and Section 5.3.

For a TT flow i, as TT frames are released for transmission selection at the offset, so:
$LA_{i\in PCF\cup TT}^p = EA_{i\in PCF\cup TT}^p = o_i^p$

Finally, the characteristic of a PTT frames are detailed in Th.9.

▶ **Theorem 9** (PTT characteristics). *A PTT frame can be characterized by a MFS, a period P, an earliest and latest arrival times, by considering different integration policies:*

$$MFS_{g\in PTT}^{p,\tau} = \begin{cases} MFS_{g\in TT},\ \textit{shuffling} \\ MFS_{g\in TT} + PO,\ \textit{preemption} \\ \Delta GB_{g\in TT}^{p} \cdot C_{out}^{p} + MFS_{g\in TT},\ \textit{guard band} \end{cases}$$

$$P_{g\in PTT}^{p,\tau} = \tau^p$$

$$EA_{g\in PTT}^{p,\tau} = \begin{cases} EA_{g\in TT}^{p,\tau},\ \textit{shuffling \& preemption} \\ EA_{g\in TT}^{p,\tau} - \Delta GB_{g\in TT}^{p},\ \textit{guard band} \end{cases}$$

$$LA_{g\in PTT}^{p,\tau} = EA_{g\in PTT}^{p,\tau}$$

where τ^p is in Eq. (5); PO is the preemption overhead size; $\Delta GB_{g\in TT}^p$ is the guard band duration of the frame $f_{g\in TT}^p$, and $g \ominus 1$ represents the frame preceding $f_{g\in TT}^p$:

$$\Delta GB_{g\in TT}^{p} = \min(\frac{MFS_{RC\cup BE}^{p}}{C_{out}^{p}}, EA_{g\in TT}^{p,\tau} - EF_{g\ominus 1\in TT}^{p,\tau})$$

with $EA_{g\in TT}^{p,\tau}$ the earliest arrival time and $EF_{g\in TT}^{p,\tau}$ the earliest finish time, of a frame g within τ^p, defined in Eq. (6) and Eq. (8).

Proof. Similarly to Th. 3, this theorem is based on the definitions of integration policies [22] and results from a direct application of the impact of integration policies on RC traffic. The full proof is detailed in the Appendix. ◀

8.2 Computation of $\alpha^p_{PCF \cup PTT}(t)$

The behavior of the $PCF \cup PTT$ flows is periodic with a period τ^p (see Eq (5)). However, a duration τ^p can start at the arrival of any frame within τ^p. We call the initial frame the "benchmark" frame. To obtain $\alpha^p_{PCF \cup PTT}(t)$, we compute the arrival curves for all benchmark frames and keep the maximum values (see Eq. (9)). As an arrival curve is due to the minimum amount of time between two arrivals of any arbitrary amount of data, we detail in Lemma 10 the minimum inter-arrival times used in Th. 11.

▶ **Lemma 10** (Minimum inter-arrival time). *We shall consider the minimum time between the arrival of benchmark frame $f^{p,\tau}_{bm} \in \{PCF, PTT\}$ and the arrival of frame $f^{p,\tau}_{bm \oplus g}$*[1]$\in \{PCF, PTT\}$*, with $g \in [0..N^{p,\tau} - 1]$ as follows:*

$$\delta^p_{bm,g} = \begin{cases} 0, \text{ if } LA^{p,\tau}_{bm} \in [EA^{p,\tau}_{bm \oplus g}, LA^{p,\tau}_{bm \oplus g}] \text{ or } LA^{p,\tau}_{bm \oplus g} \in [EA^{p,\tau}_{bm}, LA^{p,\tau}_{bm}] \\ EA^{p,\tau}_{bm \oplus g} - LA^{p,\tau}_{bm}, \text{ otherwise} \end{cases}$$

with $EA^{p,\tau}_{bm \oplus g}$ and $LA^{p,\tau}_{bm \oplus g}$ the arrival times of $f^{p,\tau}_{bm \oplus g}$ (see Eq. (6), Eq. (7) and Th. 9).

Proof. We divide our analysis in two parts: we consider 1) never overlapping arrivals; 2) potentially overlapping arrivals:

1) *never overlapping arrivals:* when considering the PTT or PCFs arriving after the latest arrival time of the PTT or PCF benchmark bm, the minimum time interval occurs when the benchmark arrives closest to the next frame, i.e. we consider the benchmark starting time to be $LA^{p,\tau}_{bm}$ and $\delta^p_{bm,g} = EA^{p,\tau}_{bm \oplus g}$- $LA^{p,\tau}_{bm}$;

2) *potentially overlapping arrivals:* two frames $f^{p,\tau}_{bm}$ and $f^{p,\tau}_{bm \oplus g}$ can overlap iif:

$LA^{p,\tau}_{bm \oplus g} \in [EA^{p,\tau}_{bm}, LA^{p,\tau}_{bm}]$ or $LA^{p,\tau}_{bm} \in [EA^{p,\tau}_{bm \oplus g}, LA^{p,\tau}_{bm \oplus g}]$

The minimum interval is when $f^{p,\tau}_{bm}$ and $f^{p,\tau}_{bm \oplus g}$ arrive at the same time, i.e. $\delta^p_{bm,g} = 0$. ◀

Knowing Lemma 10, the arrival curve of the aggregate PCF and PTT flow is as follows.

▶ **Theorem 11** (Arrival curve of $PCF \cup PTT$ traffic). *The arrival curve of $PCF \cup PTT$ traffic in output port p is:*

$$\alpha^p_{PCF \cup PTT}(t) = \max_{bm \in \{0..N^{p,\tau}-1\}} \left\{ \alpha^{p,bm}_{PCF \cup PTT}(t) \right\} \tag{9}$$

with arrival curve of the $PCF \cup PTT$ flow when considering benchmark frame $f^{p,\tau}_{bm}$ such as:

$$\alpha^{p,bm}_{PCF \cup PTT}(t) = \sum_{g \in \{0..N^{p,\tau}-1\}} \alpha^p_{g \in PCF \cup PTT}(t - \delta^p_{bm,g})$$

where $N^{p,\tau}$ and $\delta^p_{bm,g}$ are defined respectively in Section 8.1 and Lemma 10, and

$$\alpha^p_{g \in PCF \cup PTT}(t) = \begin{cases} MFS^{p,\tau}_{g \in PCF \cup PTT} \cdot \left\lceil \frac{t + LA^p_i - EA^p_i}{\tau^p} \right\rceil, t > 0 \\ 0, t \leqslant 0 \end{cases}$$

is the arrival curve of frame $f^{p,\tau}_g$ of flow $i \in \{PCF, PTT\}$ with a maximum arrival jitter $LA^p_i - EA^p_i$ (defined in Eq. (6), Eq. (7) and Th. 9), a period τ^p (see Eq. (5)), a MFS such as $MFS^{p,\tau}_{g \in PTT}$ is defined in Th. 9 and $MFS^{p,\tau}_{g \in PCF} = MFS_{PCF}$ (see Th. 4).

[1] $f^{p,\tau}_{bm \oplus g}$, the g-th frame after a benchmark frame $f^{p,\tau}_{bm}$

Proof. For $\alpha^{p}_{PCF \cup PTT}(t)$, the proof is identical to the proof of Eq. (12) in [22]. For $\alpha^{p,bm}_{PCF \cup PTT}(t)$, the proof is similar to the proof of Theorem 2 in [22], with two differences, i) because of Lemma 10, we consider here $\delta^{p}_{bm,g}$ instead of the relative offsets between benchmark frame and adjacent frames; ii) because of the IW, we must also consider the arrival jitter $LA^{p}_{i} - EA^{p}_{i} > 0$ in the arrival curve $\alpha^{p}_{g \in PCF \cup PTT}(t)$, rather than $LA^{p}_{i} - EA^{p}_{i} = 0$ like in [22] (due to having only fixed scheduling time instants in [22]). ◀

9 Performance Evaluation

We start by presenting the case study. Then, we present the results of the impact of PCFs on TT and RC traffic.

9.1 Case Study

We study a realistic adaptation of the Orion CEV use case, the 100 Mbps network described in [19, 22] and illustrated in Fig. 2. The TT and RC flows are defined in [22] in Table 2 (MFS without preamble, start of frame delimiter, interframe gap or necessary padding to reach the minimum frame size). We define for the synchronization a level-2 synchronization redundancy. We consider one RC class and the RC initial jitter is null. The PCF flows are as follows: one flow from each CM to the SMs and SCs, one flow from each SM to the CMs. The TT schedule is generated using the SMT-based approach proposed in [14, 5].

We consider linear arrival curves described in Section 5.1 and staircase service curves resulting from Th. 2 with the arrival curves described in Th. 11, as explained in Section 5.3.

We consider the following delays: the compression master delay $\Delta CM = 25.040\ \mu s$, the propagation delay = 5 ns and the forwarding delays in an end-system es: $\Delta^{es}_{fwd} = 2.44\ \mu s$, $\delta^{es}_{fwd} = 1.38\ \mu s$; and in a switch sw: $\Delta^{sw}_{fwd} = 11.45\ \mu s$, $\delta^{sw}_{fwd} = 9.22\ \mu s$.

Concerning the PCFs characteristics, we study two values for IC: an average value, i.e. 10 ms, and a small value, i.e. 1 ms. The corresponding calculated values of the network precision [18] (for the following hardware: ^{TTE} End System A664 Lab and ^{TTE} Switch A664 Lab) are respectively ϵ=4 μs for IC=1 ms and ϵ=6.7 μs for IC=10 ms. To study the impacts of IC and ϵ separately, we define 3 use cases: UC_1={IC=1 ms & ϵ=4 μs}, UC_2={IC=10 ms & ϵ=4 μs}, UC_3={IC=10 ms & ϵ=6.7 μs}. In the case of the impact of PCFs on RC, we consider a fourth use case: UC_4={IC=1 ms & ϵ=5 μs}, where the selected precision is slightly larger than the minimum achievable precision.

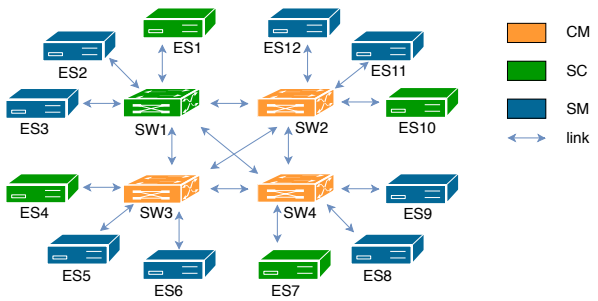

Figure 2 Case study: network description.

9.2 Impact of PCFs on TT

In this section, we compute the end-to-end delay, jitter and reserved bandwidth impacts defined in Section 7.1 without PCFs and with PCFs for both the current method and the proposed mitigation method: *improved TT Sending Window* method, applied to all the TT flows. We also study the impact of our mitigation method on the computation time. We consider two TT integration policies: shuffling and guard band. Depending on the TT flow constraints, a guard band may be automatically activated by the scheduler.

9.2.1 Minimum worst-case end-to-end delay

Our aim is to find the minimum worst-case end-to-end delay achievable using deadline constraints, 1) without PCF; 2) with PCF for the current method; 3) with PCF for the mitigation method, denoted respectively 1) *without*, 2) *current* and 3) *mitigate* in Table 2. For the case *without* PCFs, we consider that a theoretical external synchronization is set up with the defined precision ϵ. The results are in Table 2 for six representative TT flow examples in terms of various MFS, periods and number of potentially interfering PCFs.

Table 2 Minimum worst-case end-to-end delays (μs).

	without PCF		UC_1 IC=1 ms ϵ=4 μs		UC_2 IC=10 ms ϵ=4 μs		UC_3 IC=10 ms ϵ=6.7 μs	
Flow	ϵ=4 μs	ϵ=6.7 μs	current	mitigate	current	mitigate	current	mitigate
TT5	55	63	96	61	96	55	104	63
TT6	223	233	276	276	276	230	287	240
TT9	408	419	460	408	460	408	472	419
TT12	65	73	98	72	98	65	107	73
TT17	385	392	419	419	419	385	426	392
TT20	79	86	132	79	132	79	141	86

First, the current PCF impact increases with the number of PCFs along the path. We note that the deltas between the results of *current* vs. *without* are coherent with Th. 6 and the number of PCFs in the path of the flows (within 1μs due integer rounding margin). For instance, there are 6 PCFs in the output ports of the path of TT5, resulting in a theoretical delta of 40.32 μs, which is coherent with the deltas of 41 μs in Table 2 for all use cases, i.e. 96-55=41 for $\epsilon = 4$ μs (i.e. UC_1 and UC_2), and 104-63=41 for $\epsilon = 6.7$ μs (i.e. UC_3).

Consequently, compared to without PCFs, the current TT end-to-end worst-case delays are increased between 8.67% and 74.5%, i.e. (426-392)/392=8.67% for TT17 with ϵ=6.7 μs, and (96-55)/55=74.5% for TT5 with ϵ=4 μs.

With the mitigation method, the impact of the PCFs on TT depends on the number of interfering PCFs and the possible delays to avoid scheduling a frame inside IWs (see Th. 6).

Firstly, in Table 2, we find that the *mitigate* values are within 1 μs of the values expected with the minimum impact of PCFs defined in Th. 6, due to integer rounding margin. For instance, for UC_1 and TT 5, there is one PCF impacting the TT flow along its path, so the minimum impact of PCF on TT is $1 \cdot 84 \cdot 8/100 = 6.724$ μs, which is coherent with the delta of *mitigate* vs. *without*: 61-55=6 μs. However, in an additional test, i.e. with TT6, UC_4={IC=1 ms & ϵ=5 μs}, we found that the *mitigate* value is +3 μs larger than the value expected with the minimum impact of PCFs, due to a delay to avoid a IW. This brings the PCF impact in the *mitigate* delay between the minimum and maximum impacts of PCFs on worst-case end-to-end delays as defined in Th. 6.

Secondly, the probability of an offset being inside a IW depends on:

1) the hyperperiod of the TT period and the PCF period (i.e. least common multiple between TT period and IC). For example for IC=1 ms and TT20, which has a period of 5 ms, each IW must be considered five times (i.e. one for each IC within the hyperperiod). For TT6, which has a period of 3.125 ms, however, each IW have to be considered 25 times. Hence, it is much more likely that the offset will fall within a IW in this second case. In fact, we can see in Table 2, in UC_1, that TT6 is impacted by all the PCFs, whereas TT20 is not impacted by any PCF;
2) when IC increases, there are less PCFs frames being sent and the intervals between the IWs increases. Thus, there are more possibilities to schedule the TT frames outside the IWs. For example, we can see in Table 2 that with UC_1, TT6 has a delay of 276 μs due to 8 interfering PCFs, whereas with UC_2, TT6 has a delay of 230 μs due to one PCFs;
3) when ϵ increases, it increases the duration of the IWs (see Th. 5). Hence, the intervals between IWs decrease, which decreases the possibility of scheduling TT outside IWs.

Also, ϵ impacts the TT end-to-end delays: when ϵ increases, the latest arrival time increases (see Lemma 7), leading to an increase of the end-to-end delays when the number of interfering PCF is constant, as illustrated in Table 2 for both *without* and *current* results.

Thus, when IC is increased to reduce the number of interfering PCFs, ϵ increases, which increases the end-to-end delays. Sometimes, the reduction of PCFs out-weights the delay increase due to the precision change, e.g. TT6 and TT17, but other times, the increase of delays are larger than the gains due to the PCF impact reduction, e.g. TT5, TT9, TT12.

Finally, we have shown that the mitigation method is effective in reducing the impact of the PCFs on the TT end-to-end delays by limiting the number PCFs interfering with TT. With the mitigation method, the impact of the PCFs varies from 0% to 22.7% with UC_1 and from 0% to 3.0% for UC_3, i.e. (276-223)/223=22.7% for TT6 with UC_1, and (240-233)/233=3.0% for TT6 with UC_3.

This represents a large improvement over the current method, where the impact of PCFs varies between 8.67% and 74.5%.

However, when implementing the mitigation method, IC must be selected carefully to manage the best trade-off between limiting the number of interfering frames and the delays due to ϵ resulting from the selected IC.

9.2.2 Maximum jitter

For flows constrained to have a very low jitter, the guard band is activated in the last output port of the path to remove the jitter due to the lower priority traffic. Thus, the jitter of a TT flow is entirely due to the higher priority shuffling. In our use case, each ES receives 3 PCFs, so the impact of the AS6802 standard on the TT flow jitter is currently equal to the transmission times of 3 PCFs, i.e. 20.164 μs. With the mitigation method, if a low jitter constraint is set, the scheduler will find a solution without PCF interfering frame in the last output port, if it exists. In our use cases, such a solution exists, hence the maximum jitter reduction is up to 100% with the mitigation method compared to the current method.

9.2.3 Reserved bandwidth

By assessing the additional bandwidth reservation due to the PCFs, we can assess the amount of bandwidth that cannot be used by other TT and thus assess the reduction the maximum TT load caused by the PCFs, We have selected the output port with the most TT flows, i.e. $[SW2, ES12]$. Without PCFs, the bandwidth reserved by the TT flows is 38.35 Mbps,

whereas with the current method, the bandwidth reserved is 42.58 Mbps, which represents an increase of 11.04%. With the mitigation method and UC_1={IC=1 ms & ϵ=4 μs}, the bandwidth reserved is 41.80 Mbps, which represents an increase of 9.00% compared to without PCFs. This increase of the reserved bandwidth is reduced down to 1.75% with UC_2={IC=10 ms & ϵ=4 μs}, and down to 2.87% with UC_3={IC=10 ms & ϵ=6.7 μs}. By increasing IC ($UC_1 \rightarrow UC_2$), we decrease the number of PCFs inside the TT period, thus decreasing the likelihood of a PCF interfering with the TT frames, leading to a reduced reserved bandwidth compared to UC_1. By increasing ϵ ($UC_2 \rightarrow UC_3$), the IWs are enlarged and thus the likelihood a PCF interfering with a TT frame increases, leading to an increased reserved bandwidth compared to UC_2.

Hence, with the mitigation and an appropriate IC, we are able to schedule more TT traffic than with the current method. In our case study, compared to the current method, we estimate that for UC_3, the increase of maximum traffic load is around 7%, which corresponds to the reduction of bandwidth reserved with the mitigation, from 42.6 Mbps to 39.45 Mbps.

9.2.4 Computation time

The improvements of the TT metrics compared to the current method are obtained at the cost of an increase of the computation time (i.e. run time of the schedule generator), which is multiplied by up to 15 times, from about 3 s to 45 s when applied to all the flows. The computation times can be drastically improved by only applying the mitigation method to very low deadline constraints, jitter constraints or highly loaded ports. For instance, for UC_1 with a deadline of 96 μs for TT5, the average computation time is 3.25 s with the current method, 3.93 s with the mitigation method only applied to TT5, and 3.91 with the mitigation method only applied to output port $[SW2, ES12]$. With a deadline of 61 μs, average computation time is 4.76 s with the mitigation method only applied to TT5. We obtain the same results as Sections 9.2.1, 9.2.2 and 9.2.3 when applying the mitigation method only on a flow or port of interest. Hence, by selectively applying the mitigation method, we are able to achieve large improvements for a low computational cost.

To conclude, the AS6802 standard has currently a large impact on the TT traffic, with an increase of the end-to-end delays up to 74.5 %, an increase of the maximum jitter from 0 to 20 μs and an increase of the reserved bandwidth of 11%, in our case study.

The mitigation method has good results in decreasing these impacts. The impact on the end-to-end delays is reduced by up to 100 % (from 8.67% to 0%), the impact on the jitter is reduced up to 100% (from 20 μs to 0 μs), and the impact on the reserved bandwidth is divided by up to 6 (from 11% to 1.75%), in the most loaded port. By reducing the reserved bandwidth, we free bandwidth for additional flows. However, the actual increase of schedulable TT flows depends on the flows added to the network, which will be explored in future work.

We have shown that selecting appropriate IC and calculating the corresponding network precision ϵ is very important to obtain the best results possible with the mitigation method. Additional work is needed to explore the trade-off between the effects of increasing IC to reduce the number of PCFs, and the effect of the resulting decrease of the network precision.

9.3 Impact of PCFs on RC

We compare the worst-case delays computed with the method proposed in the paper, with the delays computed using the method described in [22], which does not consider PCFs. Then we discuss the effects of the PCF parameters, mitigation method and scheduler on RC.

9.3.1 Impact for a fixed schedule and fixed (IC, ϵ)

The TT integration policy guard band is set for all flows in all ports. The deltas between RC worst-case delays without (modeled from [22]) and with (see Th. 11) PCF traffic for UC_4 are detailed in Fig. 3. The RC flows are generally multicast and their worst-case delays are presented individually by destination: for an RC flow X, with a destination ESY, the flow is denoted $X.Y$. For instance, 2.7 refers to flow RC 2, from ES4 to ES7.

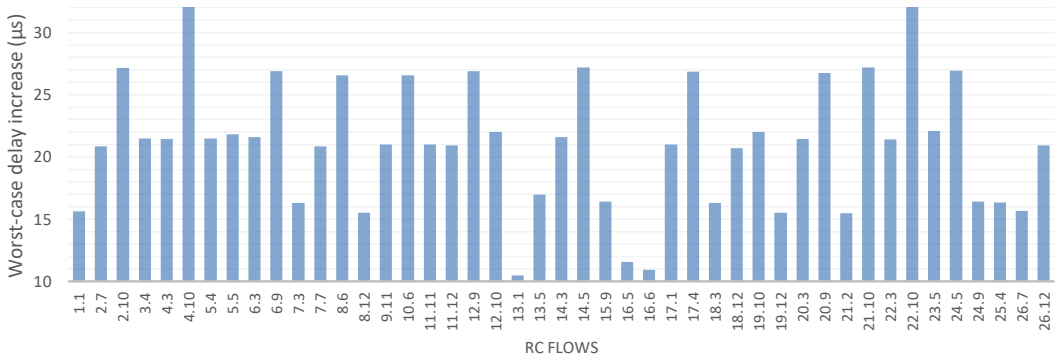

Figure 3 RC worst-case delay increase with PCF (Th. 11), compared to without PCF (cf. [22]) for UC_4.

Results show that for UC_4={IC=1 ms & ϵ=5 μs}, the RC delays are increased between 10.49 μs and 32.56 μs (or between 0.55 % and 1.99 %) by the added PCF traffic. This increase depends mainly on the number of PCFs in the RC flow path: e.g. an increase of about i) 11 μs is due to 3 PCFs, ii) 21 μs is due to 5 PCFs, iii) 32 μs is due to 7 PCFs. For instance, for RC flow 16.6 between ES4 and ES6, there are 3 PCFs along the path and the worst-case delay is increased by 10.91 μs. For RC flow 4.10 between ES9 and ES10, there are 7 interfering PCFs, and the worst-case delay is increased by 32.56 μs. The increase also depends on the IW placements with regard to the TT schedule. For example, both RC 13.5 and RC 1.1 encounter 4 PCFs, but the worst-case delay increases by 16.98 μs for RC 13.5, and by 15.61 μs for RC 1.1.

To conclude, in this experiment the PCFs increase the worst-case delay of the RC traffic (up to 32.56 μs or 1.99%), depending on the number of PCFs in the path and the interactions between IWs and TT offsets. Hence, not taking PCFs into account may lead to optimistic bounds and result in an unsafe system.

9.3.2 Discussion: impact of (IC, ϵ)

When IC increases, the number of PCFs in a hyperperiod decreases, which decreases the arrival curve of the $PCF \cup TT$ traffic (see Th. 11). So, the impact $PCF \cup TT$ traffic decreases and the RC delays are smaller.

As presented in Section 9.2.3, IW is larger when ϵ increases. Hence, in Lemma 10, the arrival window of a PCF is larger. Consequently, it is more likely for the minimum inter-arrival times to be equal to 0, which increases the arrival curve of the $PCF \cup TT$ traffic. So, the impact $PCF \cup TT$ traffic increases and the RC delays are larger.

Hence, when IC increases and ϵ is constant, the RC delays decrease. When IC is constant and ϵ is increases, the RC delays increase.

As increasing of IC also increases the corresponding minimum ϵ, selecting a correct couple (IC, ϵ) is to find a good balance between the two effects of IC and ϵ, similarly to the effects discussed in Section 9.2.1.

9.3.3 Discussion: impact of mitigation method and schedule generator

The mitigation method computes differently the TT sending windows. As such, the schedule selected by the chosen solver may be different with the mitigation method compared to without. However, the impact is only due to the different selected offsets. Hence, the selection of a different schedule generator could have a similar impact. In this evaluation, we have selected an SMT solver, but our mitigation method could be applied with other solutions. So comparing the solution with and without mitigation method is similar to comparing different schedules obtained by different schedule generators, which, while interesting, is not the objective of this paper.

10 Conclusion

In this paper, we have proposed a novel Network Calculus model of the Protocol Control Frame (PCF) defined in the AS6802 synchronization protocol. Using this model, we have computed the impact of the PCF traffic on the Time-Triggered (TT) traffic. In particular, we proposed a method to reduce the impact of PCFs, by improving the TT Sending Window computation. Moreover, we have used the PCF model to compute a novel Network Calculus model of both TT and PCF traffic to assess the impact on Rate-Constrained (RC) traffic.

Our test results show that with the current method, the impact of the PCFs on TT represents an increase of up to 74.5% of the end-to-end delays, up to 11% of the reserved bandwidth, and up to 20 μs of the maximum jitter. We have also shown that the PCF traffic increases the RC worst-case delays, up to 32.56 μs or 1.99% in our case study. Hence, PCFs must be taken into account to obtain correct worst-case delays for RC traffic and ensure a safe system.

Finally, in our case study, with our proposed mitigation method, i.e. improved TT Sending Windows method, we obtain a reduction of the impact of the PCFs on TT on the end-to-end delay (up to 100%), jitter (up to 100%) and reserved bandwidth (up to 6 times) compared to the current method. Throughout the evaluation, we have showed that finding the correct tuple (IC, ϵ) is of paramount importance to obtain good performances and reduce the impact of PCFs on TT and RC.

In future work, we plan to further study the impact of the integration cycle and network precision on both the mitigation method and on the impact of PCFs on RC and TT, and to validate the mitigation method on a larger industrial network.

References

1 Airlines Electronic Engineering Committee. Aircraft Data Network Part 7, Avionics Full Duplex Switched Ethernet (AFDX) Network, ARINC Specification 664. In *Aeronautical Radio*, 2002.

2 Anne Bouillard, Laurent Jouhet, and Eric Thierry. Service curves in Network Calculus: dos and don'ts. Research report, INRIA, 2009.

3 M. Boyer, H. Daigmorte, N. Navet, and J. Migge. Performance impact of the interactions between time-triggered and rate-constrained transmissions in TTEthernet. In *European Congress on Embedded Real Time Software and Systems*, 2016.

4 Marc Boyer, Jörn Migge, and Nicolas Navet. An efficient and simple class of functions to model arrival curve of packetised flows. In *Proc. of the 1st Int. Workshop on Worst-Case Traversal Time (WCTT)*, 2011.

5 Silviu S. Craciunas and Ramon Serna Oliver. Combined task- and network-level scheduling for distributed time-triggered systems. *Real-Time Systems*, 52(2):161–200, 2016.

6 J. Diemer, D. Thiele, and R. Ernst. Formal worst-case timing analysis of Ethernet topologies with strict-priority and AVB switching. In *Proc. International Symposium on Industrial Embedded Systems (SIES)*. IEEE Computer Society, 2012.

7 Fabrice Frances, Christian Fraboul, and Jérôme Grieu. Using network calculus to optimize the AFDX network. In *Embeeded Real Time Software and Systems (ERTS)*, 2006.

8 Jérôme Grieu. *Analyse et évaluation de techniques de commutation Ethernet pour l'interconnexion des systèmes avioniques*. PhD thesis, INPT, 2004.

9 Hermann Kopetz, Astrit Ademaj, Petr Grillinger, and Klaus Steinhammer. The Time-Triggered Ethernet (TTE) Design. *8th IEEE International Symposium on Object-oriented Real-time distributed Computing (ISORC), Seattle, Washington*, 2005.

10 J.Y. Le Boudec and P. Thiran. *Network calculus: a theory of deterministic queuing systems for the internet*. Springer-Verlag, 2001.

11 SAE International. SAE AS6802 Time-Triggered Ethernet. `http://standards.sae.org/as6802/`, 2011.

12 Miladin Sandić, Ivan Velikić, and Aleksandar Jakovljević. Calculation of number of integration cycles for systems synchronized using the AS6802 standard. In *2017 Zooming Innovation in Consumer Electronics International Conference (ZINC)*, pages 54–55. IEEE, 2017.

13 Eike Schweissguth, Peter Danielis, Dirk Timmermann, Helge Parzyjegla, and Gero Mühl. ILP-based joint routing and scheduling for time-triggered networks. In *Proceedings of the 25th International Conference on Real-Time Networks and Systems*, pages 8–17. ACM, 2017.

14 Wilfried Steiner. An Evaluation of SMT-based Schedule Synthesis For Time-Triggered Multi-Hop Networks. In *RTSS*. IEEE, 2010.

15 Wilfried Steiner. Synthesis of static communication schedules for mixed-criticality systems. In *2011 14th IEEE International Symposium on Object/Component/Service-Oriented Real-Time Distributed Computing Workshops*, pages 11–18. IEEE, 2011.

16 Wilfried Steiner, Günther Bauer, Brendan Hall, and Michael Paulitsch. TTEthernet: Time-Triggered Ethernet. In Roman Obermaisser, editor, *Time-Triggered Communication*. CRC Press, August 2011.

17 Wilfried Steiner and Bruno Dutertre. Automated formal verification of the TTEthernet synchronization quality. In *NASA Formal Methods Symposium*, pages 375–390. Springer, 2011.

18 Wilfried Steiner and Bruno Dutertre. The TTEthernet synchronisation protocols and their formal verification. *International Journal of Critical Computer-Based Systems 17*, 4(3):280–300, 2013.

19 Domitian TamasSelicean, Paul Pop, and Wilfried Steiner. Timing analysis of rate constrained traffic for the TTEthernet communication protocol. In *2015 IEEE 18th International Symposium on Real-Time Distributed Computing*, pages 119–126. IEEE, 2015.

20 Daniel Thiele, Philip Axer, and Rolf Ernst. Improving formal timing analysis of switched ethernet by exploiting FIFO scheduling. In *Proceedings of the 52nd Annual Design Automation Conference*, page 41. ACM, 2015.

21 L. X. Zhao, H. G. Xiong, Z. Zheng, and Q. Li. Improving worst-case latency analysis for rate-constrained traffic in the time-triggered ethernet network. *IEEE Communications Letters*, 18(11):1927–1930, 2014.

22 Luxi Zhao, Paul Pop, Qiao Li, Junyan Chen, and Huagang Xiong. Timing analysis of rate-constrained traffic in TTEthernet using network calculus. *Real-Time Systems*, 53(2):254–287, 2017.

A Appendix

A.1 Proof of Theorem 5: PCF Integration Window

Proof. To compute a IW, i.e. $EA^p_{i \in PCF}$ and $LF^p_{i \in PCF}$, we need to consider when a frame can arrive in the output port *psrc* of a source node, i.e. between the earliest arrival time

($EA^{psrc}_{i\in PCF}$) and the latest arrival time ($LA^{psrc}_{i\in PCF}$). We must also consider the delays $\delta^{[src,n]}_{i\in PCF}$ and $\Delta^{[src,n]}_{i\in PCF}$ defined in Section 5.3, and the precision of the network synchronization ϵ:

$EA^{p}_{i\in PCF} = EA^{psrc}_{i} + \delta^{[src,n]}_{i} - \epsilon$ and $LF^{p}_{i\in PCF} = LA^{psrc}_{i} + \Delta^{[src,n]}_{i} + \Delta^{p}_{i} + \epsilon$.

It is necessary to consider ϵ since EA^{psrc}_{i} and LA^{psrc}_{i} are from the point of view of the local time of the source node, while EA^{p}_{i} and LF^{p}_{i} are from the point of view of the local time of p. Next, we compute EA^{psrc}_{i} and LA^{psrc}_{i} for the different PCF origins.

PCFs from SM to CM: the PCFs of flow i sent by the SMs are released for transmission selection at the beginning of each IC. Each IC starts at local time 0, thus:

$EA^{psrc}_{i\in PCF} = LA^{psrc}_{i\in PCF} = 0$.

PCFs from CM to SM and SC: to compensate for the asymmetric reception of PCFs (due to different path sizes for example), AS6802 implements the so-called *permanence function* inside the CMs. This service function applies a delay to the PCF reception times equal to the statically computed worst-case travel time of any PCF in the network (called the *maximum transparent clock* MTC), ensuring that the CMs process the PCFs according to the PCFs release times, rather than reception time. For this, each PCF accumulates its travel time in its *transparent clock* TC field, which is increased at each intermediate hop it traverses. Upon arrival of a frame at time t_A in the CM input port, the $permanence function$ computes the delta between the maximum transparent clock MTC and the transparent clock TC, denoted δ_{TC}. Then, it delays the delivery of the PCF to the CM host until the expiration of this delta. When the frame is delivered, it is said to become *permanent*. This so-called permanent time also depends on δ_{clock}, the clock drift between the values of the clock of the source and the clock of the destination, as the sending time is from the point of view of the source and the permanent time is from the point of view of the destination.

Hence, the permanent time is: $t_A + \delta_{TC} = TC + \delta_{clock} + MTC - TC = \delta_{clock} + MTC$.

The maximum (resp. minimum) value of the clock drift δ_{clock} (and consequently the value of the clock compensation delay) is equal to $+\epsilon$ (resp. $-\epsilon$).

Next, the CM compute the clock compensation delay, during a known Compression Master delay ΔCM. Then, after taking into account the clock compensation, it sends the PCFs to the SMs and CMs.

So, we obtain: $EA^{psrc}_{i\in PCF} = -\epsilon + MTC + \Delta CM$ and $LA^{psrc}_{i\in PCF} = +\epsilon + MTC + \Delta CM$ ◀

A.2 Proof of Theorem 9: Policed Time-Triggered Frames

Proof. With shuffling, the TT frame is delayed until the lower priority frame (RC or BE) finishes its transmission. Hence, the earliest arrival time EA and the maximum frame size MFS of a PTT frame remain the same as EA and MFS of the corresponding TT frame.

With guard band (GB), a RC or BE frame is blocked from transmission if a TT frame is scheduled to be sent before the RC frame would complete its transmission. The length of the guard band before a TT frame can be upper bounded by either the maximal transmission time of a lower priority frame, i.e. RC or BE, competing on the output port p, or the idle time distance with the previous TT frame. Thus, the guard band duration of $f^{p,\tau}_{g}$ is:
$\Delta GB^{p}_{g\in TT} = \min(\frac{MFS^{p}_{RC\cup BE}}{C^{p}_{out}}, EA^{p,\tau}_{g\in TT} - EF^{p,\tau}_{g\ominus 1\in TT})$, where $g \ominus 1$ represents the frame preceding $f^{p,\tau}_{g}$. As the guard band only appears immediately before the TT frame, and RC∪BE frames are delayed by both guard bands and TT frames, it is assumed that "GB+TT" is taken as an entirety. So, we have a new MFS and a new earliest arrival time:
$MFS^{p,\tau}_{g\in PTT} = MFS_{g\in TT} + \Delta GB^{p}_{g\in TT} \cdot C^{p}_{out}$ and $EA^{p,\tau}_{g\in PTT} = EA^{p,\tau}_{g\in TT} - \Delta GB^{p}_{g\in TT}$, with $g \in PTT$ when considering the TT frame $f^{p,\tau}_{g}$ with the integration policy, $g \in TT$ without the integration policy.

With preemption (PR), even though the lower priority frame is preempted by a TT frame, the TT frame will suffer a delay of the fixed-sized preemption overhead PO. As the PO postpones and appears immediately before the TT frame, we assume an entirety "PR+TT" of PTT which impacts on RC traffic. Then, PTT ("PR+TT") obtains the same earliest arrival time as TT and $MFS^{p,\tau}_{g\in PTT} = MFS_{g\in TT} + PO$.

All three integration policies have a fixed impact on the arrival time of a PTT frame, and a TT frame is always released by the device to the output port p at $EA^{p,\tau}_{g\in TT}$. Hence, $LA^{p,\tau}_{g\in TT} = EA^{p,\tau}_{g\in TT}$ and the period is τ^p. ◀